The Chodura layer formation in an active and collisional plasma under the action of a constant magnetic field

2016 Plasma Sources Sci. Technol. 25 025019

(http://iopscience.iop.org/0963-0252/25/2/025019)

IOP Publishing Plasma Sources Science and Technology

Plasma Sources Sci. Technol. **25** (2016) 025019 (13pp) doi:10.1088/0963-0252/25/2/025019

The Chodura layer formation in an active and collisional plasma under the action of a constant magnetic field

R Morales Crespo

Departamento de Física, Universidad de Córdoba, Campus Universitario de Rabanales, Ed. C2. 14071 Córdoba, Spain

E-mail: rutphysics@gmail.com

Received 23 October 2015, revised 4 January 2016
Accepted for publication 21 January 2016
Published 29 February 2016

Abstract

This paper studies the multi-layer structure of the plasma-sheath transition for an electropositive plasma under the action of a constant and oblique magnetic field. The introduction of the Chodura-scale allows us to introduce the concepts of *Chodura-layer*, *Chodura-edge* and *Chodura-solution* in a natural way as a consequence of a boundary layer structure formalism—in a similar manner to what happens in the plasma-sheath transition. Therefore, the region from the plasma bulk to the wall can be divided in three regions: (i) the plasma-presheath, a quasineutral space region dominated by ionization and/or collisions, (ii) the Chodura-layer, a quasineutral region also dominated by the action of the magnetic field though the drift term and finally (iii) the sheath region. It is shown that if magnetization is the dominant presheath mechanism, it is only located in the Chodura-layer, and this causes the electric field to become singular at the Chodura-edge, between two quasineutral regions—i.e. the plasma-presheath and the Chodura-layer.

Keywords: Chodura layer, sheath, magnetic presheath

(Some figures may appear in colour only in the online journal)

1. Introduction

The interaction of a limited plasma with a solid wall is a problem that has been widely studied since the early works of Langmuir [1]. Nowadays, the number of papers that study this plasma-surface transition are increasing due to the very important role it plays in many applications [2]. Some of these applications include surface treatment in the electronic industry applied to semiconductor fabrication, the interaction of spacecraft with surrounding space plasmas, the use of conducting surfaces for plasma diagnostics, or in the case of a magnetized plasma, the edge of magnetically confined fusion plasmas. The characterization of these plasma boundaries, which determines particle and energy losses from the plasma, allows us to improve manufacturing processes, to get to know some of the discharge properties and to interpret the corresponding measurements.

Among these applications, many papers describing the features of the transition that occurs when a plasma is in contact with a conducting surface under the action of a constant magnetic field have been published in recent years. Among these works is the pioneering paper of Chodura [3], which describes the magnetic presheath of a collisionless and non-active plasma under the action of a magnetic field. According to this model, Chodura shows that before the sheath, there is a magnetic-presheath, called the Chodura-layer, characterized because at the entrance of this layer, the positive ions become supersonic in the direction of the magnetic field. Along the Chodura-layer, the electric field increases, causing the motion of the positive ions to deviate from the magnetic field direction and increasing their perpendicular velocity to the wall. This causes a change in the supersonic character of the ion motion from the magnetic field lines to the normal wall direction. When the positive ions are supersonic in the direction perpendicular to the wall, the sheath edge has been reached. Riemann [4] extends the model to include collisions when the magnetic field is almost parallel to the wall. Ahedo [5]

considered the influence of the magnetic field strength and the angle of incidence of the magnetic field. Stangeby [6] sees a contradiction in the existence of a sheath-edge where the ion velocity normal to the wall becomes supersonic, and the Chodura-layer characterized by an edge (in the following, the Chodura-edge) where the ion velocity parallel to the magnetic field also becomes supersonic—both edges being related to a singularity in the electric field. This contradiction would arise from the fact that while the sheath-edge separates a quasineutral region from a space-charged one (the sheath), the Chodura-edge would separate two quasineutral regions—the 'plasma-presheath' and the 'magnetic-presheath' or the Chodura-layer. Sternberg-Poggie [7] and Hutchinson [8] assert that the Chodura-layer and the alignment of ion motion along the magnetic field is a mathematical artefact that disappears when collisions and ionization are included in the model—unlike what happens with the Bohm criterion which persists in any case. According to [7], in the models of [4] and [8] the positive ions would be aligned to the magnetic field only in the case of a very strong field in the centre of the plasma, in which case, not only would the presheath be magnetized, but also the sheath. Finally, in recent years, several authors [9–15] have claimed that a new Bohm criterion for a plasma under the action of a constant magnetic field is derived when collisions are considered together with magnetization.

The present work develops the model published by Crespo and Franklin [16] corresponding to the plasma-sheath transition close to a planar wall in a plasma submitted to a constant magnetic field where all the possible presheath mechanisms—i.e. collisions, ionization and magnetization through the drift term $\mathbf{E}\times\mathbf{B}$—are present. Although this model provides the mathematical tools to study the features of the plasma-sheath transition in the whole range of collisionality, ionization, and magnetization, this paper is focused on the special case where magnetization corresponds to the prevailing presheath mechanism in the description of the ion dynamics towards the sheath—i.e. the case where the ion gyroradius $\lambda_b = c_s M_+/eB$ is smaller than both the mean free path for collisions λ_c and ionization λ_i. In section 2 we present the equations of the model. In section 3, they are normalized according to the four characteristic lengths of the problem, i.e. the Debye length $\lambda_D = (\varepsilon_0 K_B T_e/en_{e0})^{1/2}$, the ion gyroradius λ_b, the mean free path for ionization λ_i, and the mean free path for the ion-neutral collisions λ_c. This would allow us to define the sheath and presheath representations and show how to solve the model for the special case where $\lambda_b = \min\{\lambda_i, \lambda_c, \lambda_b\}$. In section 4 we introduce the Chodura-representation, characterized by a new length scale—the Chodura-scale—defined by $\bar{\lambda} = \min\{\lambda_i, \lambda_c\}$. This representation introduces a new parameter $\bar{q} = \lambda_b/\bar{\lambda}$, called the *non-collinearity* parameter, which gives us an idea of the deviation of ion motion with respect to the magnetic field lines for the case $\lambda_b/\bar{\lambda} \to 0$.

The advantage of the Chodura representation is that it naturally introduces the three concepts of Chodura-layer, Chodura-edge, and Chodura-solution in a similar way to the sheath, sheath-edge and sheath-solution according to a mathematical structure of the boundary layer, which relates two physical descriptions in two different scale lengths. In this sense, if the sheath-edge separates a quasinetural region (presheath) from a space-charged one (sheath), the Chodura-edge corresponds to the point that separates two quasineutral regions—the first one where the ions are trapped by the magnetic field lines (plasma-presheath) and the second one where they begin to deviate from the magnetic field direction (Chodura-layer). Although these two regions are both quasineutral, they are characterized by two different length scales that cause a singularity in the electric field at that point when $\lambda_b/\bar{\lambda} \to 0$—in the same way that the transition from the presheath to the sheath causes a singularity in the electric field when $\lambda_D/\lambda_b \to 0$. Therefore, the singularity in the electric field in the transition from the plasma-presheath to the Chodura-layer is not related to a breakdown of quasineutrality but a breakdown of the collinearity of ion velocity with respect to the magnetic field due to the drift term $\mathbf{E}\times\mathbf{B}$.

According to the above discussion, the transition from the plasma bulk to the wall comprises the following three regions: (i) the plasma-presheath, a quasineutral space region where ion dynamics are dominated by collisions and/or ionization, ending this region at the Chodura-edge, (ii) from this point to the sheath-edge, there is the Chodura-layer (or 'magnetic-presheath')—also a quasineutral region according to its own length scale but with a high electric field according to the plasma-presheath scale or Chodura-scale. The electric field in the Chodura-layer is not high enough to break down the quasineutrality, but it is enough to influence ion motion through the drift term $\mathbf{E}\times\mathbf{B}$, causing them to deviate from the magnetic field lines towards the normal wall direction. This region ends at the sheath-edge, (iii) and finally beyond this point to the wall there is the sheath.

Contrary to Stangeby [6], the quasineutrality of both regions (the plasma-presheath and the Chodura-layer) does not imply any contradiction to the fact that ions move supersonically and aligned to the magnetic field in the Chodura-edge and the existence of a singularity in the electric field—because this singularity is due to the mathematical boundary layer structure of these two regions. From a physical point of view, as shown in section 4.5, this happens because although $\lambda_b < \lambda_i$ and $\lambda_b < \lambda_c$, being λ_b the scale of the total presheath (in the following $\lambda_b = \lambda$), the magnetic presheath mechanism is not present in the whole range from the plasma bulk to the sheath-edge. This mechanism is only located and important in the Chodura-layer, where the drift term $\mathbf{E}\times\mathbf{B}$ begins to increase due to the increase of the electric field. Before the Chodura-layer, the only presheath mechanisms that exist are ionizations and collisions. In this sense, there are two different physical presheath mechanisms (ionization/collisions on the one hand and magnetization on the other) acting on the two separated regions. These are characterized with a very different length scale, which causes a boundary layer structure and therefore a singularity in the electric field in the transition from one region to the other. This explains why there is no multilayer structure when the main presheath mechanism is collisions or ionization. As these mechanisms do not depend on the electric field or the magnetic field, they are uniformly distributed in the whole presheath, from the plasma bulk to the sheath edge.

In this section, we also investigate the thickness of the three regions which separate the plasma bulk from the wall, when $\lambda_D \ll \lambda \ll \bar{\lambda}$ being $\lambda = \lambda_b$ and $\bar{\lambda} = \min\{\lambda_c, \lambda_i\}$. We find that the plasma-presheath thickness is of the order of $\bar{\lambda}$, the Chodura-layer thickness scales as $\lambda^{1-t}\bar{\lambda}^t$, where $0 < t < 1$, and finally the sheath thickness scales as $\lambda_D^h \lambda^{-h}\bar{\lambda}$ where $0 < h < 1$. Once we have solved the equations of the model and obtained the numerical solutions, the thickness of the Chodura-layer and the sheath region can be fitted considering $t = 2/5$ and $h = 4/5$—i.e. the Chodura-layer scales as $\lambda^{3/5}\bar{\lambda}^{2/5}$, and the sheath as $\lambda_D^{4/5}\lambda^{-4/5}\bar{\lambda}$.

In section 4.3 we also study the behaviour of the electric field in the neighbourhood of the Chodura-edge and the sheath-edge. We show that near the sheath-edge, the electric field is proportional to $\lambda_D^{r-1}\lambda^{-r}$ where $0 < r < 1$ and this allows us to show that the concept of a modified Bohm criterion (claimed by the above-mentioned authors) for forming a positive sheath disappears when the dependence of the electric field on λ_D/λ is considered. In the case of the Chodura-edge, it is shown that the electric field scales as $\lambda^{s-1}\bar{\lambda}^{-s}$ where $0 < s < 1$, and this helps us to explain how the drift term $\mathbf{E} \times \mathbf{B}$ disappears in the plasma-presheath when $\lambda/\bar{\lambda} \to 0$—i.e. the magnetic presheath mechanism through the drift term does not act on the plasma-presheath, it is only located in the Chodura-layer. This is, therefore, contrary to Sternberg [7], in the sense that the ions move in the plasma-presheath region trapped by the magnetic field lines even for a weak magnetic field that, in any case, would not cause a magnetized sheath.

2. The model

In a hydrodynamic framework, the equations for describing the motion of the positive ions in the plasma-sheath transition for a negatively polarized wall immersed in a plasma under the action of a constant oblique magnetic field lying in a plane perpendicular to the wall are: (i) the continuity equation

$$\nabla \cdot (n_+ \mathbf{v}_+) = \nu_i n_e \tag{1}$$

and (ii) the momentum transfer equation:

$$M_+ n_+ (\mathbf{v}_+ \cdot \nabla \mathbf{v}_+) + \nu_c M_+ n_+ \mathbf{v}_+ + \nu_i M_+ n_e \mathbf{v}_+ = e n_+ (\mathbf{E} + \mathbf{v} \times \mathbf{B}) \tag{2}$$

n_+, $\mathbf{v}_+$, $\mathbf{E}$, $\mathbf{B}$, ν_i, ν_c being the positive ion density, the positive ion velocity, the electric field, the magnetic field, the ionization frequency, and the collision frequency respectively. We will consider the *YOZ*-plane parallel to the wall and the *X*-direction perpendicular to it, and therefore the electric and magnetic fields are written as $\mathbf{E} = E\mathbf{e}_x$ and $\mathbf{B} = B(\cos\theta \mathbf{e}_x + \sin\theta \mathbf{e}_y)$.

The validity of the Boltzmann relation for the electrons when there is a magnetic field parallel to the wall has been re-examined by several authors [17, 18]. If the electron current flowing to the sheath is very small [17] or $v^2/c_s^2 \ll m_e/M$ (where v is the electron flow velocity, c_s the Bohm velocity and m_e, M the mass of the electrons and ions respectively) this relation is valid. Zimmermann *et al* [18] show that in a coaxial discharge with an axial magnetic field, the validity of Boltzmann's relation for the electrons depends on different parameters of the plasma. When the electron Hall parameter given by $eB_\parallel/m_e\nu_{ce}$ is small enough, the Boltzmann relation:

$$n_e = n_{e0} e^{e\phi/K_B T_e}, \tag{3}$$

is still valid, T_e and n_{e0} being the electron temperature and the electron density in the plasma bulk, ν_{ce} corresponding to the non-ionizing collision rate for the electrons, and $B_\parallel$ being the axial magnetic field parallel to the wall. For values of the electron Hall parameter around 10, only if the ionization rate is small can the Boltzmann relation be used. Finally, for greater values of the electron Hall parameter, the error created by the use of the Boltzmann relation is too big to be considered. In the following, we consider the more restrictive case for which the non-ionizing collision mean free path for the electrons is very small compared to the electron gyroradius ($c_s/\nu_{ce} \ll c_s m_e/eB$). If we express the parallel component of the magnetic field as $B_\parallel = B\sin\theta$, the electron Hall parameter as stated in [18] is small enough in order for equation (3) to be valid.

Finally, there is also the Poisson equation, which determines the electric potential profile from the plasma to the wall:

$$\nabla^2 \phi = -\frac{e}{\varepsilon_0}(n_+ - n_e) \tag{4}$$

where ϕ is the electric potential referred to the plasma potential.

Due to the symmetry of the problem, we consider that all our variables depend only on the perpendicular coordinate to the wall—i.e. the x-coordinate—the origin of the coordinates being in the centre of the plasma, located to the left of the wall.

If we express the ion-neutral collision frequency as $\nu_c(v_+) = n_n c_s \sigma_s (v_+/c_s)^{p+1}$, where n_n is the density of the neutrals and σ_s is the collisional cross section when $v_+ = c_s = \sqrt{K_B T_e/M_+}$ (the Bohm velocity), the constant collision frequency case would correspond to $p = -1$, while the constant mean free path case would correspond to $p = 0$. From now on, in the major part of this paper, we will consider the case of constant collision frequency [4].

3. Normalized model equations

There are four length scales in the model: (i) the mean free path for collisions λ_c, (ii) the mean free path for ionization λ_i, (iii) the magnetic length λ_b, and (iv) the Debye length. The last one corresponds to the size of the sheath and the other three are present in the total presheath mechanism and are defined as:

$$\lambda_c = \frac{c_s}{\nu_c(c_s)} = \frac{1}{n_n \sigma_s}, \quad \lambda_i = \frac{c_s}{\nu_i}, \quad \lambda_b = \frac{c_s M_+}{eB}. \tag{5}$$

As usual, to make all the physical constants present in the model equal one, the following quantities will be used in order to define the standard of the physical magnitudes for normalizing the equations of the model: the electron thermal energy $K_B T_e$ and its density in the plasma n_{e0}, the Bohm speed c_s, and the characteristic length of the region described as L, where $L = \lambda_D$ for the sheath region or $L = \lambda$ for the presheath

region, λ being the length scale of the presheath defined by $\lambda = \min\{\lambda_i, \lambda_c, \lambda_b\}$. Below, we will see that there is another length scale—the Chodura-scale. With all of that, the normalized electric potential, ion density, and ion velocity are $-e\phi/K_B T_e$, $N = n_+/n_{e0}$, and $\mathbf{c} = \mathbf{v}_+/c_s$, where $\mathbf{c} = (u, v, w)$ and u, v, and w are the normalized Cartesian components of the positive ion velocity. Finally, the normalization of the space coordinates with L will define what is called a representation.

3.1. The sheath representation

The characteristic length scale of the sheath corresponds to the Debye length, i.e. $L = \lambda_D$. The sheath representation determining the electric potential $\phi = \phi(x)$ in the sheath scale is defined by:

$$X = \frac{x}{\lambda_D}, \qquad y(X) = -\frac{e}{k_B T_e}\phi(\lambda_D X). \tag{6}$$

The normalized model equations according to this representation are:

$$\nabla_X(N\mathbf{c}) = q_i e^{-y}, \tag{7a}$$

$$(\mathbf{c}\cdot\nabla_X)\mathbf{c} - \nabla_X y = q_b \mathbf{c}\times\mathbf{b} - q_c|\mathbf{c}|^{p+1}\mathbf{c} - q_i\frac{e^{-y}}{N}\mathbf{c}, \tag{7b}$$

$$\nabla_X^2 y = N - e^{-y}, \tag{7c}$$

where $\mathbf{b} = (\cos\theta, \sin\theta, 0)$ is a unitary vector co-lineal to the magnetic field, $|\mathbf{c}| = (u^2 + v^2 + w^2)^{1/2}$, and q_i, q_c, and q_b are the source parameters of the three mechanisms present in the presheath region defined by:

$$q_i = \frac{\lambda_D}{\lambda_i}, \qquad q_c = \frac{\lambda_D}{\lambda_c}, \qquad q_b = \frac{\lambda_D}{\lambda_b}. \tag{8}$$

From (7*a*)–(7*c*) we can express the electric potential as $y = y(X; q_i, q_c, q_b)$. The sheath-solution, simply denoted by y_0, would correspond to $q_b = 0$, $q_i = 0$, $q_c = 0$—i.e. $y_0(X) = y(X;0, 0, 0)$, and considering that all the magnitudes only depend on X, (7*a*)–(7*c*) become:

$$(N\dot{u}) = 0, \tag{9a}$$

$$u\dot{u} - \dot{y}_0 = 0, \tag{9b}$$

$$\ddot{y}_0 = N - e^{-y_0}, \tag{9c}$$

$$v = w = 0, \tag{9d}$$

where a dot means differentiation with respect to X. The sheath-solution is universal in the sense that it does not depend on any source presheath parameter to form the sheath.

3.2. presheath representation

The presheath representation, which determines the electric potential profile $\phi = \phi(x)$ in the presheath scale is given by:

$$\xi = \frac{x}{\lambda}, \qquad \eta(\xi) = -\frac{e}{k_B T_e}\phi(\lambda\xi), \tag{10}$$

where $\lambda = \min\{\lambda_i, \lambda_c, \lambda_b\}$. In this case, the dimensionless equations of the model can be written as:

$$\nabla_\xi(N\mathbf{c}) = f_i e^{-\eta}, \tag{11a}$$

$$(\mathbf{c}\nabla_\xi)\mathbf{c} - \nabla_\xi\eta = f_b\mathbf{c}\wedge\mathbf{b} - f_c|\mathbf{c}|^{p+1}\mathbf{c} - f_i\frac{e^{-\eta}}{N}\mathbf{c}, \tag{11b}$$

$$q^2\nabla_\xi^2\eta = N - e^{-\eta}, \tag{11c}$$

where q is the non-neutrality parameter:

$$q = \lambda_D/\lambda \tag{12}$$

and f_i, f_c and f_b are defined by:

$$f_i = \frac{\lambda}{\lambda_i}, \qquad f_c = \frac{\lambda}{\lambda_c}, \qquad f_b = \frac{\lambda}{\lambda_b}. \tag{13}$$

If we define the Knudsen parameters for ionizations and collisions:

$$\beta_i = \frac{\lambda_b}{\lambda_i}, \qquad \beta_c = \frac{\lambda_b}{\lambda_c} \tag{14}$$

f_i, f_c, and f_b can be expressed as functions of β_i and β_c, according to [16]. From now on we will consider the particular case for which magnetization is the dominant presheath mechanism, i.e. $\lambda_b < \lambda_i$ and $\lambda_b < \lambda_c$, and therefore $\lambda = \lambda_b$. Nevertheless, we will use the symbol λ to refer to the presheath length scale instead of λ_b for the sake of the symmetry of the notation when we discuss the Chodura-layer. For this particular case, $f_i = \beta_i$, $f_c = \beta_c$, $f_b = 1$, and the scalar version of (11*a*)–(11*c*) are:

$$(Nu)' = \beta_i e^{-\eta}, \tag{15a}$$

$$uu' - \eta' = -b_y w - \beta_c|\mathbf{c}|^{p+1}u - \beta_i\frac{e^{-\eta}}{N}u, \tag{15b}$$

$$uv' = b_x w - \beta_c|\mathbf{c}|^{p+1}v - \beta_i\frac{e^{-\eta}}{N}v \tag{15c}$$

$$uw' = (b_y u - b_x v) - \beta_c|\mathbf{c}|^{p+1}w - \beta_i\frac{e^{-\eta}}{N}w \tag{15d}$$

$$q^2\eta'' = N - e^{-\eta}, \tag{15e}$$

where prime denotes derivation with respect to ξ, and $b_x = \cos\theta$, $b_y = \sin\theta$.

The solution of (15*a*)–(15*e*) can be written as $\eta = \eta(\xi; q, \beta_i, \beta_c)$. The plasma-solution or presheath-solution that will be written as η_0, would correspond to the case $q = 0$, i.e. from (15*e*) $N = e^{-\eta_0}$ and therefore $\eta_0 = \eta(\xi; 0, \beta_i, \beta_c)$.

$$u' - \eta_0' u = \beta_i, \tag{16a}$$

$$uu' - \eta_0' = -b_y w - (\beta_c|\mathbf{c}|^{p+1} + \beta_i)u, \tag{16b}$$

$$uv' = b_x w - (\beta_c|\mathbf{c}|^{p+1} + \beta_i)v \tag{16c}$$

$$uw' = (b_y u - b_x v) - (\beta_c|\mathbf{c}|^{p+1} + \beta_i)w \tag{16d}$$

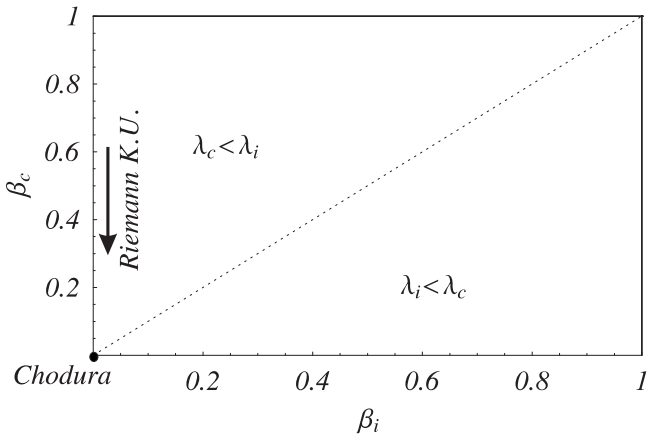

Figure 1. $\beta_\mathrm{i} \times \beta_\mathrm{c}$ plane for a magnetic presheath where $\lambda_\mathrm{b} = \min\{\lambda_\mathrm{b}, \lambda_\mathrm{i}, \lambda_\mathrm{c}\}$ and therefore $0 \leqslant \beta_\mathrm{i} \leqslant 1$, and $0 \leqslant \beta_\mathrm{c} \leqslant 1$. The point (0, 0) would correspond to the original Chodura model. In the same way, the ordinate axis would correspond to the model of a magnetic presheath only influenced by collisions (Riemann [4]).

$$N = \mathrm{e}^{-\eta_0}. \tag{16e}$$

Unlike the sheath-solution y_0 which is independent of the three source presheath parameters q_b, q_i, and q_c, the presheath-solution η_0 is independent of the non-neutrality parameter $q = q_\mathrm{b}$, but depends on the other two β_i and β_c. In this sense, we say the non-neutrality parameter q gives us an idea of the deviation of the electric potential η from the quasineutral solution η_0 for the realistic case $\lambda_\mathrm{D}/\lambda \neq 0$. The parameters β_i and β_c determine the degree of influence of ionization and collisions in the formation of the magnetized presheath. If the influence of ionization in the presheath formation increases, then β_i increases; if the influence of collisions increases, then β_c increases too. Figure 1 (see [16]) represents a Cartesian $\beta_\mathrm{i} \times \beta_\mathrm{c}$ plane which depicts the two regions that correspond to the two cases considered in this paper, i.e. $\lambda_\mathrm{b} < \lambda_\mathrm{i} < \lambda_\mathrm{c}$ and $\lambda_\mathrm{b} < \lambda_\mathrm{c} < \lambda_\mathrm{i}$.

The presheath-solution η_0 can be used to obtain the initial conditions to integrate the model (15*a*)–(15*e*) and solve the electric potential profile from the plasma to the wall $\eta(\xi; q, \beta_\mathrm{i}, \beta_\mathrm{c})$ for the more realistic case $q = \lambda_\mathrm{D}/\lambda_\mathrm{b} \neq 0$ by assuming the quasineutrality condition close to the centre of the plasma, i.e. $\eta \simeq \eta_0$ and $\eta' \simeq \eta_0'$ at $\xi \to 0$.

From the presheath-solution, the sheath-edge would correspond to the point where the ions become supersonic in the x-direction normal to the wall, and the electric field has a singularity $\eta_0' \to \infty$. Indeed, from (16*b*) we can obtain u', and substituting into (16*a*) yields:

$$\eta_0' = \frac{(2\beta_\mathrm{i} + \beta_\mathrm{c}|\mathbf{c}|^{p+1})u + b_y w}{1 - u^2} \tag{17}$$

which becomes infinite at the point where $u = 1$ (Bohm criterion).

3.3. Numerical solution of the model

For any $q \neq 0$, the initial conditions to solve (15*a*)–(15*e*) can be obtained assuming that in the plasma bulk, ($\xi \to 0$) where quasineutrality holds and ions are at rest ($\mathbf{c} \to 0$) the following approximations are accurate: $\eta \simeq \eta_0 \to 0$, $\eta' \simeq \eta_0' \to 0$, and $N \simeq \mathrm{e}^{-\eta_0}$. The following series expansions can therefore be tried:

$$u = u_1\xi + \cdots, \tag{18a}$$

$$v = v_1\xi + \cdots, \tag{18b}$$

$$w = w_1\xi + \cdots, \tag{18c}$$

$$\eta = \eta_0 = \eta_{02}\xi^2 + \cdots, \tag{18d}$$

$$\eta' = \eta_0' = 2\eta_{02}\xi + \cdots, \tag{18e}$$

where u_1, v_1, w_1, and η_{02} are constants to be determined. By substituting these expressions on (16*a*)–(16*d*) and taking into account the first terms different from zero, we finally get:

$$u_1 = \beta_\mathrm{i}, \tag{19a}$$

$$v_1 = \frac{\beta_\mathrm{i} b_x b_y}{(2\beta_\mathrm{i} - p\beta_\mathrm{c})^2 + b_x^2}, \tag{19b}$$

$$w_1 = \frac{\beta_\mathrm{i}(2\beta_\mathrm{i} - p\beta_\mathrm{c})b_y}{(2\beta_\mathrm{i} - p\beta_\mathrm{c})^2 + b_x^2}, \tag{19c}$$

$$\eta_{02} = \frac{\beta_\mathrm{i}(2\beta_\mathrm{i} - p\beta_\mathrm{c})}{2}\left(1 + \frac{b_y^2}{(2\beta_\mathrm{i} - p\beta_\mathrm{c})^2 + b_x^2}\right). \tag{19d}$$

To build up the initial conditions and solve the whole model from the plasma to the wall, we only have to choose a sufficiently small value of u—let us call it u_i—in order for ξ at that point to fulfil $\xi \to 0$ (close to the plasma centre), i.e. $\xi_\mathrm{i} = u_\mathrm{i}/u_1 \to 0$, where u_i is the only arbitrary parameter. Once we have selected the u_i value, the initial conditions to solve (15*a*)–(15*e*) are built up from (18*a*)–(18*e*) in the form $u_\mathrm{i} = u(\xi_\mathrm{i})$, $v_\mathrm{i} = v(\xi_\mathrm{i})$, $w_\mathrm{i} = w(\xi_\mathrm{i})$, $\eta_\mathrm{i} = \eta(\xi_\mathrm{i})$, $\eta_\mathrm{i}' = \eta'(\xi_\mathrm{i})$ and $N_\mathrm{i} = \mathrm{e}^{-\eta_\mathrm{i}}$. For instance, let us suppose that for a plasma with a constant collision frequency ($p = -1$), $\lambda_\mathrm{b} = 4\lambda_\mathrm{D}$, $\lambda_\mathrm{i} = 10\lambda_\mathrm{b}$, $\lambda_\mathrm{i} = 5\lambda_\mathrm{c}$ and the magnetic field has $\theta = \pi/3$, then it yields:

$$\left.\begin{array}{l}\lambda_\mathrm{b} = 10\lambda_\mathrm{D}\\ \lambda_\mathrm{i} = 10\lambda_\mathrm{b}\\ \lambda_\mathrm{i} = 5\lambda_\mathrm{c}\\ \theta = \pi/3\\ p = -1\end{array}\right\} \Rightarrow \left\{\begin{array}{l}\beta_\mathrm{i} = 0.1\\ \beta_\mathrm{c} = 0.5\\ b_x = \cos(\pi/3)\\ b_y = \sin(\pi/3)\end{array}\right\} \Rightarrow \left\{\begin{array}{l}u_1 = 0.1\\ v_1 = 0.058\,5152\\ w_1 = 0.081\,9213\\ \eta_{02} = 0.070\,473\end{array}\right\} \Rightarrow \tag{20}$$

now, if we take a very small value of u to consider that we are close to the centre of the plasma, for instance $u_\mathrm{i} = 10^{-8}$, then:

$$\xi_\mathrm{i} = \frac{u_\mathrm{i}}{u_1} = \frac{10^{-8}}{0.1} = 10^{-7} \Rightarrow \left\{\begin{array}{l}v_\mathrm{i} = v_1\xi_\mathrm{i} = 5.851\,52 \cdot 10^{-9}\\ w_\mathrm{i} = w_1\xi_\mathrm{i} = 8.192\,13 \cdot 10^{-9}\\ \eta_\mathrm{i} = \eta_{02}\xi_\mathrm{i}^2 = 7.0473 \cdot 10^{-16}\\ \eta_\mathrm{i}' = 2\eta_{02}\xi_\mathrm{i} = 1.409\,46 \cdot 10^{-8}\end{array}\right\} \tag{21}$$

and finally, we can write the initial conditions as: $u(10^{-7}) = 10^{-8}$, $v(10^{-7}) = 5.851\,52 \cdot 10^{-9}$, $w(10^{-7}) = 8.192\,13 \cdot 10^{-9}$, $\eta(10^{-7}) = \eta(10^{-7}) = 7.0473 \cdot 10^{-16}$, $\eta'(10^{-7}) = 1.409\,46 \cdot 10^{-8}$.

4. The Chodura-representation

Although the main presheath mechanism we are considering is magnetization, the presheath region is also characterized by the parameters β_i and β_c, which determine the degree of ionization and collisionality present in the plasma. To describe this feature of the magnetic presheath, we define a new length scale $L = \bar{\lambda} = \min\{\lambda_i, \lambda_c\}$. This length will define the Chodura-representation by:

$$\zeta = x/\bar{\lambda}, \qquad \tau(\zeta) = -\frac{e}{k_B T_e}\phi(\bar{\lambda}\zeta). \tag{22}$$

Following the same mathematical treatment as in section 3.2 to define the presheath representation for the most general case, we will define the parameter $\bar{q} = \lambda/\bar{\lambda} = \max\{\beta_i, \beta_c\}$, and from this, the functions:

$$\bar{f}_i = \frac{\bar{\lambda}}{\lambda_i}, \qquad \bar{f}_c = \frac{\bar{\lambda}}{\lambda_c} \tag{23}$$

or

$$\bar{f}_i(\beta_{ic}) = \begin{cases} 1, & \lambda_i < \lambda_c \\ \beta_{ic}, & \lambda_i > \lambda_c \end{cases} \tag{24a}$$

$$\bar{f}_c(\beta_{ic}) = \begin{cases} 1/\beta_{ic}, & \lambda_i < \lambda_c \\ 1, & \lambda_i > \lambda_c \end{cases} \tag{24b}$$

where $\beta_{ic} = \beta_i/\beta_c$.

The parameter $\bar{q}$, the functions $\bar{f}_i$, $\bar{f}_c$ and the parameter β_{ic}, play the same mathematical role as q, the functions f_b, f_c, f_c, and β_i, β_c respectively in the presheath-representation with a different physical meaning. To understand this physical meaning, we write the equations of the model in the Chodura-representation as:

$$\nabla_\zeta(N\mathbf{c}) = \bar{f}_i e^{-\tau}, \tag{25a}$$

$$(\mathbf{c}\cdot\nabla_\zeta)\mathbf{c} - \nabla_\zeta\tau = \frac{1}{\bar{q}}\mathbf{c}\wedge\mathbf{b} - \bar{f}_c|\mathbf{c}|^{p+1}\mathbf{c} - \bar{f}_i\frac{e^{-\tau}}{N}\mathbf{c}, \tag{25b}$$

$$q^2\bar{q}^2\nabla_\zeta^2\tau = N - e^{-\tau}. \tag{25c}$$

Considering that $\lambda = \min\{\lambda_b, \lambda_i, \lambda_c\}$, and $\bar{\lambda} = \min\{\lambda_i, \lambda_c\}$, it is straightforward to see that $\bar{q} < 1$ and the more restrictive condition for obtaining quasineutrality is $q \to 0$. If we write (25*a*)–(25*c*) in the form:

$$\nabla_\zeta(N\mathbf{c}) = \bar{f}_i e^{-\tau}, \tag{26a}$$

$$\bar{q}\left\{(\mathbf{c}\cdot\nabla_\zeta)\mathbf{c} - \nabla_\zeta\tau + (\bar{f}_c|\mathbf{c}|^{p+1} + \bar{f}_i\frac{e^{-\tau}}{N})\mathbf{c}\right\} = \mathbf{c}\wedge\mathbf{b}, \tag{26b}$$

$$q^2\bar{q}^2\nabla_\zeta^2\tau = N - e^{-\tau}, \tag{26c}$$

we see that if the parameter q gives an idea of the deviation of the electric potential profile from the quasineutral-solution according to (11*c*) and (26*c*), the parameter $\bar{q}$—in the following called the non-collinearity parameter—gives us an idea of how much the ion velocity $\mathbf{c}$ deviates from the magnetic field direction $\mathbf{b}$, according to (26*b*). In the limit $q \to 0$, the quasineutrality-solution η_0 is obtained, but in the limit $\bar{q} \to 0$ (where $\mathbf{b}$ and $\mathbf{c}$ are colinear vectors) the Chodura-solution is obtained (which corresponds to a particular presheath-solution). For the general case, the solution of (26*a*)–(26*c*) can be expressed as $\tau = \tau(\zeta; q, \bar{q}, \beta_{ic})$ and therefore the Chodura-solution would be written as $\tau_0(\zeta; \beta_{ic}) = \tau(\zeta; 0, 0, \beta_{ic})$.

All three representations mentioned throughout this paper are related by:

$$\zeta = \bar{q}\xi = \bar{q}qX \qquad y(X; q_i, q_c, q_b) = \eta(\xi; q, \beta_i, \beta_c) = \tau(\zeta; q, \bar{q}, \beta_{ic}). \tag{27}$$

4.1. The Chodura-solution

To obtain the Chodura-solution, the two limits $q \to 0$ and $\bar{q} \to 0$ are considered. First, in (26*a*)–(26*c*) we take the limit $q \to 0$ to get the presheath or plasma-solution for which $N = e^{-\tau}$. In this case, the scalar form of these equations would be written as:

$$\dot{u} - \dot{\tau}u = \bar{f}_i, \tag{28a}$$

$$\bar{q}(u\dot{u} - \dot{\tau}) = -b_y w - \bar{q}(\bar{f}_i + \bar{f}_c)u, \tag{28b}$$

$$\bar{q}u\dot{v} = b_x w - \bar{q}(\bar{f}_i + \bar{f}_c)v, \tag{28c}$$

$$\bar{q}u\dot{w} = (b_y u - b_x v) - \bar{q}(\bar{f}_i + \bar{f}_c)w \tag{28d}$$

where dot now means differentiation with respect to ζ. Substituting the $\dot{\tau}$ and w obtained from (28*a*) and (28*c*) respectively into equation (28*b*), the above equations will transform in:

$$\dot{u} - \dot{\tau}u = \bar{f}_i, \tag{29a}$$

$$(u - \frac{1}{u})\dot{u} = -\frac{b_y}{b_x}(u\dot{v} + (\bar{f}_i + \bar{f}_c)v) - \bar{f}_c u - \bar{f}_i(u + \frac{1}{u}), \tag{29b}$$

$$\bar{q}u\dot{v} = b_x w - \bar{q}(\bar{f}_i + \bar{f}_c)v, \tag{29c}$$

$$\bar{q}u\dot{w} = (b_y u - b_x v) - \bar{q}(\bar{f}_i + \bar{f}_c)w. \tag{29d}$$

Finally, if we consider the limiting case $\bar{q} \to 0$, from (29*c*) and (29*d*) we obtain $w = 0$ and $v = b_y u/b_x$ respectively, and taking into account that $b_x^2 + b_y^2 = 1$ we get:

$$\dot{\tau}_0 = \frac{2\bar{f}_i + \bar{f}_c}{b_x^2 - u^2}u, \tag{30a}$$

$$\dot{u} = \frac{(\bar{f}_i + \bar{f}_c)u^2 + b_x^2\bar{f}_i}{b_x^2 - u^2}, \tag{30b}$$

$$v = \frac{b_y}{b_x} u \tag{30c}$$

$$w = 0 \tag{30d}$$

where $\tau_0 = \tau(\zeta; 0, 0, \beta_{ic})$ is the Chodura-solution. We conclude from these equations that in the limiting case where $q \to 0$ and $\bar{q} \to 0$, the first derivative of the electric potential and the x-component of the ion velocity are singular at $u = b_x$. This corresponds to the case described by Chodura [3] in the original paper, because according to (30*c*) for $u = b_x$ it yields $v = b_y$ and the ion velocity parallel to the magnetic field becomes supersonic:

$$c_{\parallel} = \mathbf{c} \cdot \mathbf{b} = b_x u + b_y v = 1 \tag{31}$$

or in physical units $v_{+\parallel} = c_s$. The point ζ_{ch}, where the electric field has a singularity and ions become supersonic in the direction of the magnetic field, determines what is called the Chodura-edge.

The Chodura-solution can be obtained integrating equations (30*a*)–(30*c*) considering that in the centre of the plasma ($\zeta = 0$), $\tau_0 = 0$ and $u = v = w = 0$. In parametric form, it is given by:

$$\tau_0(\bar{u}) = \left(\frac{a+b}{2b}\right) \ln(a + b\bar{u}^2), \tag{32a}$$

$$\bar{\zeta}(\bar{u}) = \frac{a+b}{\sqrt{ab^3}} \tan^{-1}\left(\sqrt{\frac{b}{a}}\,\bar{u}\right) - \frac{\bar{u}}{b}, \tag{32b}$$

$$\bar{v}(\bar{u}) = \bar{u}, \tag{32c}$$

$$\bar{w}(\bar{u}) = 0 \tag{32d}$$

where for the sake of simplicity we have written:

$$\bar{\zeta} = \frac{\zeta}{b_x}, \quad \bar{u} = \frac{u}{b_x}, \quad \bar{v} = \frac{v}{b_y}, \quad \bar{w} = w, \quad a = \bar{f}_i, \quad b = \bar{f}_i + \bar{f}_c. \tag{33}$$

When q and $\bar{q}$ are small, from the plasma to the point ζ_{ch}, we have the plasma-presheath region, which has a collisional or ionizing character depending on the ratio $\beta_{ic} = \beta_i/\beta_c$. In this region, the electric potential can be approximated by the Chodura solution $\tau_0(\zeta; \beta_{ic})$, which only depends on the relation of the two lengths λ_i and λ_c being independent of the parameters q and $\bar{q}$. From the point ζ_{ch} to the point $\zeta_s = \bar{q}\xi_s$, we have the Chodura-layer, where the electric potential can be approximated by the presheath-solution $\eta_0(\xi; \beta_i, \beta_c)$, which is independent of the parameter q. If we consider that $\beta_i = \bar{q}\bar{f}_i(\beta_{ic})$ and $\beta_c = \bar{q}\bar{f}_c(\beta_{ic})$, we can even express the parametric dependence of the presheath-solution as $\eta_0(\xi; \bar{q}, \beta_{ic})$. In any case, it only depends on the three lengths λ_b, λ_i, and λ_c. Finally, from ζ_s to the wall $\zeta_p = \bar{q}\xi_p = q\bar{q}x_p$ we have the sheath region which is described by the complete solution $\tau(\zeta; q, \bar{q}, \beta_{ic})$, which depends on q, $\bar{q}$, and β_{ic}—i.e. the four lengths λ_D, λ_b, λ_i and λ_c. As will be shown in section 4.2, the thickness of each one of these three regions depends on the above-mentioned lengths.

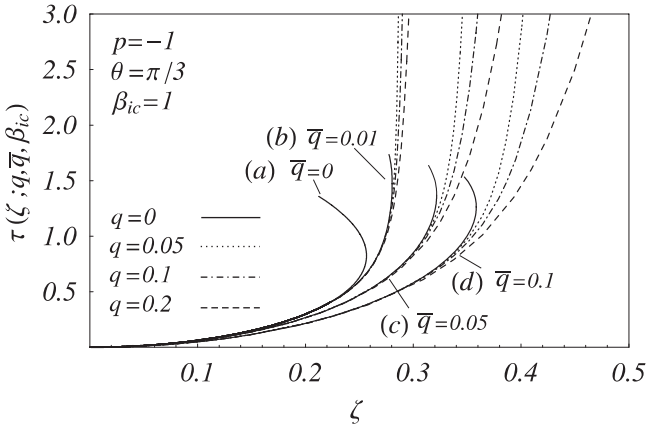

Figure 2. Presheath-solution for $\bar{q} = 0$ (also called the Chodura-solution), $\bar{q} = 0.01$, 0.05, and 0.1. For each of the last three values of $\bar{q}$ we also depict the complete solution corresponding to $q = 0.05$, 0.1, and 0.2.

To illustrate these regions, figure 2 represents the Chodura-solution $\tau_0(\zeta; \beta_{ic})$, the presheath-solution $\eta_0(\xi; \bar{q}, \beta_{ic})$ and the complete solution $\tau(\zeta; q, \bar{q}, \beta_{ic})$ for several values of $\bar{q}$ and q. Curve (*a*) depicts the Chodura-solution that corresponds to $\bar{q} = 0$, while curves (*b*), (*c*), and (*d*) correspond to the presheath-solution for $\bar{q} = 0.01$, 0.05, 0.1, respectively. Finally, for each one of these three presheath curves, we represent the complete solution for the cases $q = 0.05$, 0.1, 0.2. For all these curves, we have considered $\beta_{ic} = 1$ (i.e. $\lambda_i = \lambda_c$). As can be observed, as long as we approach the Chodura model proposed in the original work ($\lambda_i \to \infty$ and $\lambda_c \to \infty$, in figure 1, this approach would correspond to the point (0, 0) by going through the path represented as a dotted line) the presheath-solution η_0 approaches the Chodura-solution τ_0 by a uniform asymptotic matching in the plasma-presheath from $\zeta = 0$ to ζ_{ch}. In the same figure, we see that if $q \to 0$, the complete solution τ shows boundary layer behaviour in the plasma-sheath transition and uniformly matches the presheath-solution η_0 in the presheath-region—i.e. from $\zeta = 0$ to ζ_s. Finally, when $q \to 0$ and $\bar{q} \to 0$ simultaneously, both the presheath and the complete solution approach the Chodura-solution.

Figure 3 represents the electric potential profile for a particular case of the parameters β_{ic}, $\bar{q}$ and q to illustrate where the Chodura-edge ζ_{ch} and the sheath-edge ζ_s are located. In the case of ζ_{ch}, this point is well defined in the limits $\bar{q} \to 0$ and $q \to 0$, as happens in the case of ζ_s for $q \to 0$. For the more realistic case where $\bar{q} \neq 0$ and $q \neq 0$, these points (where $u = b_x$ and $u = 1$ are fulfilled respectively) are denoted as $\zeta_{\parallel}$ and ζ_C and they are obtained from the complete solution τ. Figure 3 also shows these points. In the limit $q \to 0$, it follows that $\zeta_C \to \zeta_s$, in the limit $\bar{q} \to 0$, it follows that points ζ_s and $\zeta_{\parallel} \to \zeta_{ch}$, and finally, in the double limit $q \to 0$ and $\bar{q} \to 0$, it follows that ζ_C, ζ_s, $\zeta_{\parallel} \to \zeta_{ch}$.

Figure 4 represents all these points as a function of the non-collinearity parameter $\bar{q}$. As can be seen, the thickness of the Chodura-layer defined by $\Delta\xi_{ch} = \zeta_s - \zeta_{ch}$ increases when $\bar{q}$ increases too. In the limit $\bar{q} \to 0$, the Chodura-layer edge ζ_{ch} matches the sheath-edge ζ_s. For the case illustrated in this figure (i.e. $\beta_{ic} = 1$ and $\theta = \pi/3$), we see that if $\bar{q} < 0.06$,

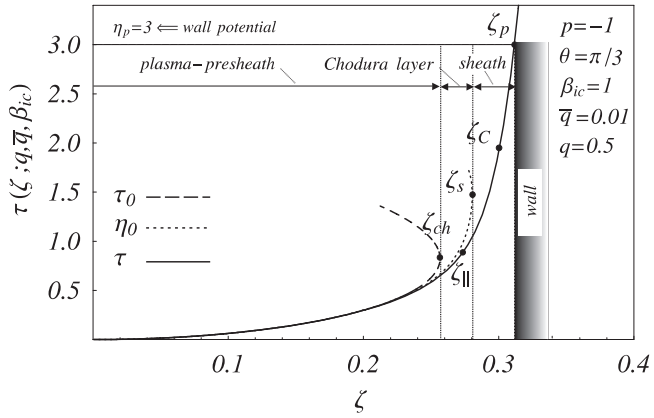

Figure 3. Illustration of the complete solution for the electric potential profile τ, the presheath solution η_0, and the Chodura-solution τ_0. The three regions from the plasma to the wall and the points ζ_{ch}, $\zeta_{\|}$, ζ_s, and ζ_C can be observed.

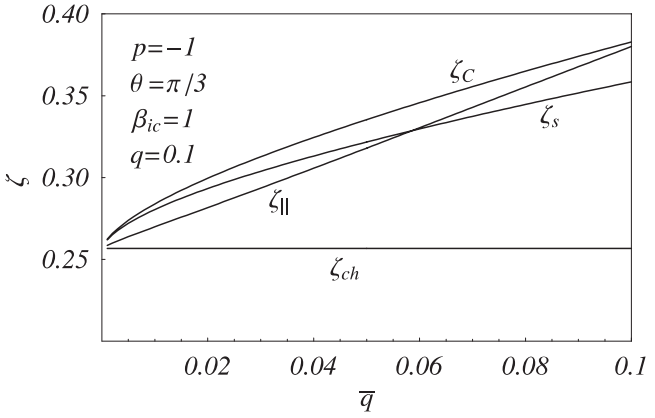

Figure 4. Representation of the Chodura-edge ζ_{ch} and the sheath-edge ζ_s for different $\bar{q}$ values. The points $\zeta_{\|}$ and ζ_C, where the ion velocity parallel to the magnetic field and the ion velocity normal to the wall reach the sound velocity are also represented.

the point $\zeta_{\|}$ where the ion velocity parallel to the magnetic field lines reaches the Bohm velocity, falls between ζ_{ch} and ζ_s, but if $\bar{q} > 0.06$, this point is located somewhere between ζ_s and ζ_C. We can also observe that the Chodura-edge location is constant $\zeta_{ch} = 0.256\,633$ or in physical units:

$$x_{ch} = 0.256\,633\bar{\lambda} = \begin{cases} 0.256\,633\lambda_i & \lambda_i < \lambda_c \\ 0.256\,633\lambda_c & \lambda_c < \lambda_i \end{cases} \tag{34}$$

Figure 5 depicts the location of the points ζ_s, $\zeta_{\|}$, and ζ_C obtained from the model with dots and depicts their corresponding analytical fit as a power series expansion of $\bar{q}^{1/5}$ with lines:

$$\zeta_s = 0.256\,503 + 0.358\,825\bar{q}^{3/5} + 0.116\,716\bar{q}, \tag{35a}$$

$$\zeta_C = 0.255\,82 + 0.402\,294\bar{q}^{3/5} + 0.259\,291\bar{q}, \tag{35b}$$

$$\zeta_{\|} = 0.257\,073 + 1.2263\bar{q}, \tag{35c}$$

from all the above expressions it can be observed that the three independent terms are almost equal to ζ_{ch}. It is straightforward to obtain the thickness of the plasma-presheath and the Chodura-layer defined by:

$$\begin{aligned} &\text{Plasma} - \text{presheath} && \Delta\zeta_{pp} = \zeta_{ch} \\ &\text{Chodura} - \text{layer} && \Delta\zeta_{ch} = \zeta_s - \zeta_{ch}. \end{aligned} \tag{36}$$

Figure 6 represents the Chodura-layer thickness according to the numerical results obtained from the model (dots) and their analytical fit (lines) in the form:

$$\Delta\zeta_{ch} = a_3\bar{q}^{3/5} + a_5\bar{q}. \tag{37}$$

4.2. Sheath-thickness

As has been shown in several papers [16, 19, 20], when q is small enough, the sheath thickness $\Delta\xi_s = \xi_p - \xi_s$ can be expressed as:

$$\Delta\xi_s = \delta_0 q^{1-m}, \tag{38}$$

where $0 \leqslant m \leqslant 1$ and ξ_p is the wall position. In the Chodura-representation this relationship would be written as:

$$\Delta\zeta_s = \bar{q}\Delta\xi_s = \delta_0\bar{q}q^{1-m}. \tag{39}$$

In general, the parameters δ_0 and m will depend on $\bar{q}$, β_{ic}, and the electric potential of the wall η_p. In the following, to study their dependence on $\bar{q}$ we will fix the wall potential and the parameter β_{ic} and therefore $\delta_0 = \delta_0(\bar{q})$ and $m = m(\bar{q})$. Figure 7 depicts the sheath-thickness in the presheath-scale with dots in the form $\lg_{10}\Delta\xi_s$ versus $\lg_{10} q$ obtained from the model for different values of the non-collinearity parameter $\bar{q}$. In the same figure, we have also represented the analytical fit according to (38) with lines:

$$\lg_{10}\Delta\xi_s = \lg_{10}\delta_0 + (1-m)\lg_{10} q, \tag{40}$$

Figure 8 represents the variation of the coefficients δ_0 and $1-m$ with $\bar{q}$ and the corresponding analytical fit:

$$\delta_0(\bar{q}) = \bar{a}_0 + \bar{a}_1\bar{q}^{1/5} + \bar{a}_2\bar{q}^{2/5} \tag{41a}$$

$$m(\bar{q}) = \bar{m}_0 + \bar{m}_1\bar{q}^{1/5} + \bar{m}_2\bar{q}^{2/5}. \tag{41b}$$

Although m is a function of the non-collinearity parameter $\bar{q}$, as can be observed in figure 7, the slope of $\lg_{10}\Delta\xi_s$ is almost constant and we can even approximate $1 - m \simeq 4/5$ or $m \simeq 1/5$; the thickness of the sheath-layer can therefore be fitted as:

$$\Delta\xi_s = \delta_0(\bar{q})q^{4/5} = \sum_{n=0} \bar{a}_n\bar{q}^{n/5}q^{4/5} \tag{42}$$

or in the Chodura-representation:

$$\Delta\zeta_s = \sum_{n=0} \bar{a}_n\bar{q}^{(n+1)/5}q^{4/5} \tag{43}$$

for instance, figure 9 represents the sheath thickness according to (42) where $\delta_0(\bar{q}) = 5.11 + 43.27\bar{q}^{1/5} - 154.50\bar{q}^{2/5} + 216.87\bar{q}^{3/5} - 144.19\bar{q}^{4/5} + 37.30\bar{q}$

With the help of (37) and (43), the wall position ζ_p, which can be obtained as the sum of the thickness of the plasma-presheath, the Chodura-layer, and the sheath is given by:

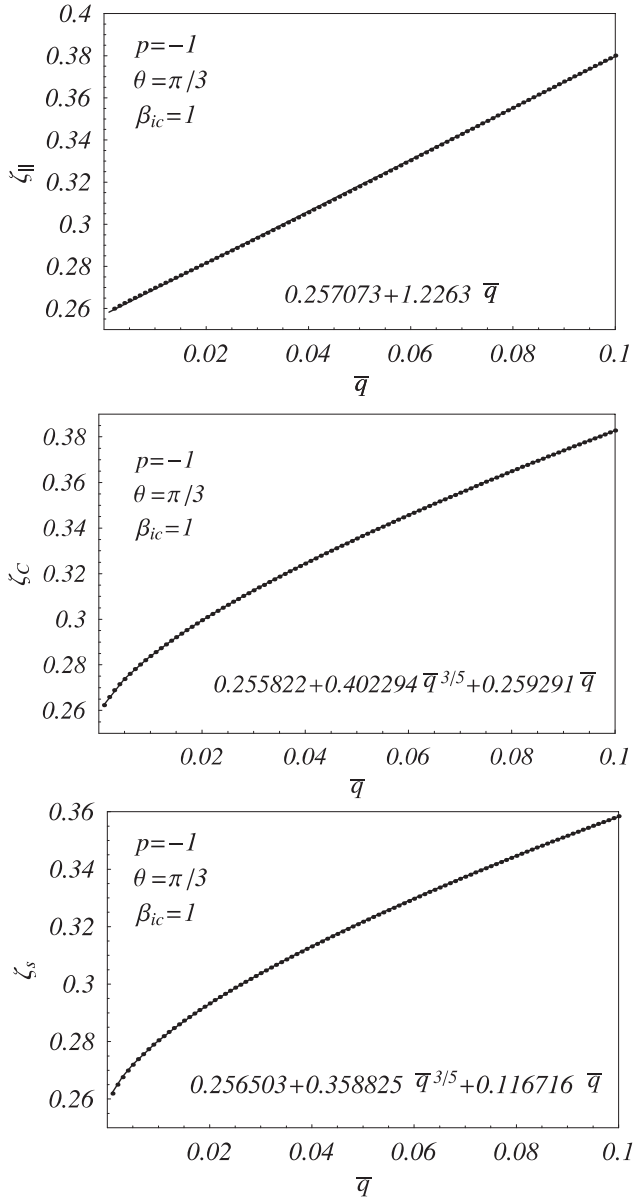

Figure 5. Location of the points $\zeta_{\parallel}$, ζ_C, ζ_s, and their analytical fit as a power series expansion $\sum_n a_n \bar{q}^{n/5}$.

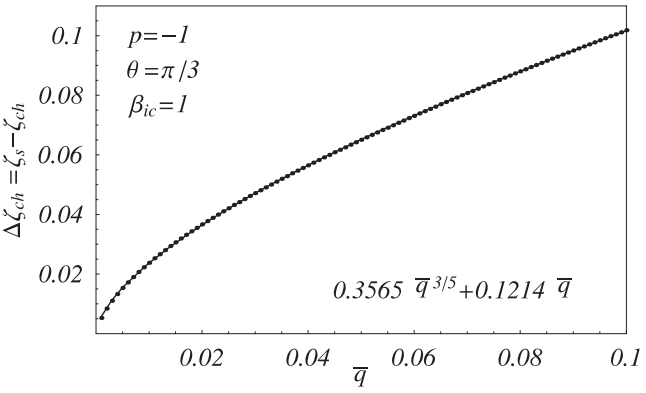

Figure 6. The Chodura-layer thickness as a function of $\bar{q}$. Dots represent the values obtained from the numerical solution of the model and the line to the analytical fit according to $\sum_n a_n \bar{q}^{n/5}$.

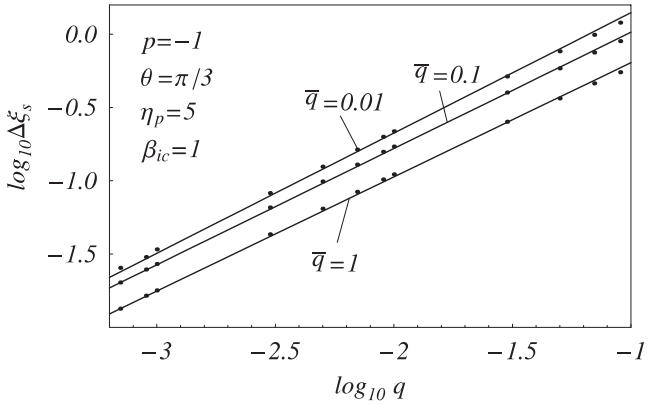

Figure 7. Sheath thickness as a function of q_b for several values of $\bar{q}$ and $\beta_{ic} = 1$. Dots represent the numerical values obtained from the model and lines represent the corresponding analytical fit according to $\Delta\xi_s = \delta_0 q_b^{1-m}$.

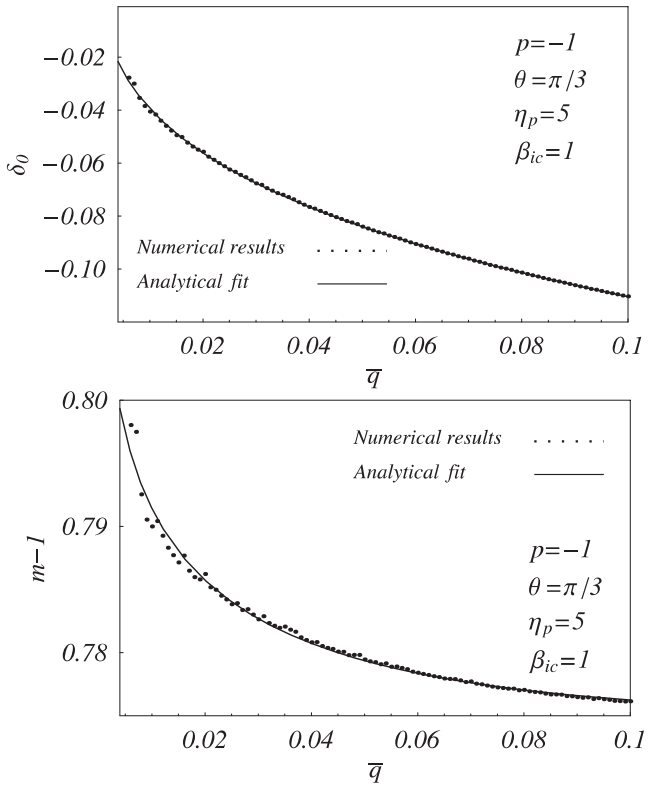

Figure 8. Parameters δ_0 and $1 - m$ as function of $\bar{q}$ and their analytical fit as a power series expansion of $\bar{q}^{1/5}$.

$$\begin{aligned}\zeta_p &= \zeta_{ch} + \Delta\zeta_{ch} + \Delta\zeta_s \\ &= \zeta_{ch} + a_3\bar{q}^{3/5} + a_5\bar{q} + (\bar{a}_0 + \bar{a}_1\bar{q}^{1/5} + \bar{a}_2\bar{q}^{2/5} + \cdots)q^{4/5} \\ &= \zeta_{ch} + a_3\bar{q}^{3/5} + \bar{a}_0 q^{4/5} + \bar{a}_1\bar{q}^{1/5}q^{4/5} + a_5\bar{q} + \bar{a}_2\bar{q}^{2/5}q^{4/5} + \cdots .\end{aligned} \tag{44}$$

If the non-neutrality parameter q and the non-collinearity parameter $\bar{q}$ are small enough, we can consider only the first three terms:

$$\zeta_p \simeq \zeta_{ch} + a_3\bar{q}^{3/5} + \bar{a}_0 q^{4/5}. \tag{45}$$

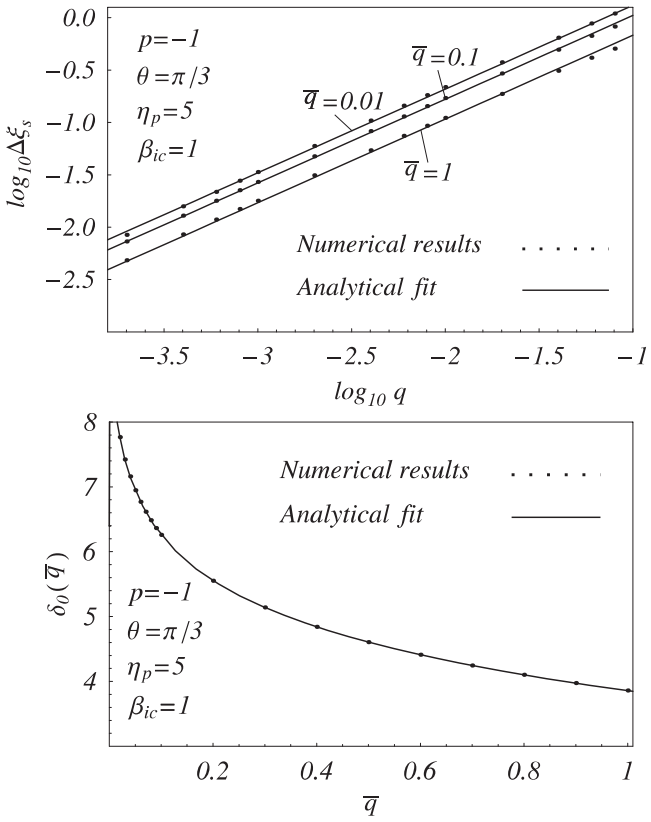

Figure 9. Analytical fit of the sheath thickness as a power series expansion in the form $\sum_n b_n q^{4/5} \bar{q}^{n/5}$.

The plasma size L corresponds to the distance from the centre of the plasma to the wall position and then $\zeta_p = L/\bar{\lambda}$ or $L = \bar{\lambda}\zeta_p$, and (45) can be expressed as:

$$L = \zeta_{ch}\,\bar{\lambda} + a_3 \lambda^{3/5}\,\bar{\lambda}^{2/5} + \bar{a}_0 \lambda_D^{4/5} \lambda^{-4/5}\,\bar{\lambda} \tag{46}$$

where $\bar{\lambda} = \min\{\lambda_i, \lambda_c\}$ and $\lambda = \lambda_b$. The first term of (46) corresponds to the size of the plasma-presheath and only depends on λ_i and λ_c; the second one, which corresponds to the Chodura-layer depends on λ_b, λ_i and λ_c; and finally the third one, which corresponds to the sheath size, depends on the four distances λ_D, λ_b, λ_i, and λ_c. L can be explicitly expressed as:

$$L = \begin{cases} \zeta_{ch}\lambda_i + a_3 \lambda_b^{3/5}\lambda_i^{2/5} + \bar{a}_0 \lambda_D^{4/5}\lambda_b^{-4/5}\lambda_i, & \lambda_i > \lambda_c \\ \zeta_{ch}\lambda_c + a_3 \lambda_b^{3/5}\lambda_c^{2/5} + \bar{a}_0 \lambda_D^{4/5}\lambda_b^{-4/5}\lambda_c, & \lambda_i < \lambda_c. \end{cases} \tag{47}$$

4.3. Electric field at the sheath edge and the Chodura layer edge

In this section, we will study the behaviour of the electric field in the three regions above described from the plasma to the wall, i.e. (i) the plasma-presheath, (ii) the magnetic-presheath or Chodura-layer and (iii) the sheath, when $\lambda_D \ll \lambda_b$, $\lambda_b \ll \lambda_i$ and $\lambda_b \ll \lambda_c$ (i.e. $q \to 0$ and $\bar{q} \to 0$), and more specifically in the neighbourhood of the Chodura-edge and the sheath-edge. This will allow us to establish two things: (i) a new formulation of the Bohm criterion for a collisional plasma, which has been claimed by several authors, does not exist, and (ii) the ion motion is aligned along the magnetic field lines as a consequence of the decrease of the drift term $\mathbf{E} \times \mathbf{B}$ when λ_b is much smaller than λ_i and λ_c, (i.e. $\bar{q} \to 0$). Or in other words, the motion of the positive ions can be aligned with the magnetic field even for a non-magnetized sheath, contrary to what was expressed by Sternberg-Poggie [7].

The electric potential profile in the three representations exposed in this paper are related by:

$$\tau(\zeta; q; \bar{q}, \beta_{ic}) = \eta(\xi; q, \beta_i, \beta_c) = y(X; q_i, q_c, q_b) \tag{48}$$

where the spatial coordinates and parameters of the three representations are related by:

Plasma − presheath	Chodura − layer	Sheath
ζ	$\xi = \bar{q}^{-1}\zeta$	$X = q^{-1}\xi$
q	q	$q_i = q\beta_i$
$\bar{q}$	$\beta_i = \bar{q}\bar{f}_i(\beta_{ic})$	$q_c = q\beta_c$
β_{ic}	$\beta_c = \bar{q}\bar{f}_c(\beta_{ic})$	$q_b = q$

(49)

and the corresponding electric field in the three representations can be expressed as:

$$q\bar{q}\partial_\zeta \tau = q\partial_\xi \eta = \partial_X y. \tag{50}$$

If we consider the case for which q and $\bar{q}$ are very small but not zero, the solution of the model $\tau(\zeta; q, \bar{q}, \beta_{ic})$ from the plasma bulk to the wall can be approximated by:

$$\tau(\zeta; q; \bar{q}, \beta_{ic}) \simeq \begin{cases} \tau_0(\zeta; \beta_{ic}), & \text{in the plasma} - \text{presheath} \quad \zeta \in (0, \zeta_{ch}) \\ \eta_0(\xi; \beta_i, \beta_c), & \text{in the Chodura} - \text{layer} \quad \zeta \in (\zeta_{ch}, \zeta_s) \\ y_0(X), & \text{in the sheath} \quad \zeta \in (\zeta_s, \zeta_p). \end{cases} \tag{51}$$

Contrary to what happens with the electric potential value, which does not depend on the representation according to (48), the electric field value will depend on the scale we use in each region. According to (50) from the plasma to the wall, the electric field can be written in the three different representations as:

In the Plasma − presheath	$\partial_\zeta \tau \simeq \partial_\zeta \tau_0 < \infty$	$\partial_\xi \eta \to 0$	$\partial_X y \to 0$
In the Chodura − layer	$\partial_\zeta \tau \to \infty$	$\partial_\xi \eta \simeq \partial_\xi \eta_0 < \infty$	$\partial_X y \to 0$
In the Sheath	$\partial_\zeta \tau \to \infty$	$\partial_\xi \eta \to \infty$	$\partial_X y \simeq \partial_X y_0 < \infty$

(52)

that is: (i) in the plasma-presheath region, the electric field is only different from zero in the Chodura-scale, (ii) in the Chodura-layer, it is zero in the sheath-scale, finite in the presheath-scale and becomes singular in the Chodura-scale as a consequence of the boundary-layer structure of the transition from the plasma-presheath to the Chodura-layer, and (iii) finally in the sheath-region, the electric field is finite in the sheath scale and becomes singular in the transition from the presheath to the sheath according to the presheath-scale and the Chodura-scale. If (52) is read vertically, it gives the variation of the electric field from the plasma bulk to the wall according to each representation.

To study how the electric field scales in the neighbourhood of the points which separate these three regions, i.e. the sheath-edge and the Chodura-edge, we will fix the wall potential value, η_p. From (38) and (39) we can estimate the electric field at the sheath-edge and the Chodura-edge (see figure 3) in the limits $q \to 0$ and $\bar{q} \to 0$ as:

$$\text{In the sheath} - \text{edge as } q \to 0 \qquad \partial_\xi \eta|_s \simeq \frac{\eta_p - \eta_s}{\Delta \xi_s} \propto q^{r-1} \tag{53a}$$

$$\text{In the Chodura} - \text{edge as } \bar{q} \to 0 \qquad \partial_\zeta \tau|_{ch} \simeq \frac{\tau_s - \tau_{ch}}{\Delta \zeta_{ch}} \propto \bar{q}^{s-1} \tag{53b}$$

where $0 < r < 1$ and $0 < s < 1$. In physical units:

$$\text{In the sheath} - \text{edge if } \lambda_D \ll \lambda_b \qquad \partial_x \phi|_s \sim \lambda_D^{r-1} \lambda_b^{-r} \tag{54a}$$

$$\text{In the Chodura} - \text{edge if } \lambda_b \ll \bar{\lambda} \qquad \partial_x \phi|_{ch} \sim \lambda_b^{s-1} \bar{\lambda}^{-s} \tag{54b}$$

Figure 10 represents the electric field at the sheath edge $\partial_\xi \eta|_s = \eta_s'$ (i.e. at point $\zeta_s = \bar{q}\xi_s$) from the complete solution of the model as a function of q and different values of $\bar{q}$. As can be observed, in the limit $q \to 0$ the electric field at ζ_s varies according to:

$$\eta_s' \propto q^{r-1} \tag{55}$$

where $0 < r < 1$, dots correspond to the numerical values and lines correspond to the analytical fit according to (55). It is clear from the above expression that if $q \to 0$, then $\eta_s' \to \infty$ in the presheath-scale—but in the sheath-scale $\partial_{xy}|_s = q\eta_s' \propto q^r \to 0$. Figure 10 also represents the electric field at ζ_C (where $u = 1$ for the complete solution τ) and we can see that it also fulfils (55).

Figure 11 represents the electric field in the Chodura-edge ξ_{ch}, i.e. $\partial_\xi \eta|_{ch} = \eta_{ch}'$ obtained by the solution of the model (dots). As can be deduced from figure 2, at this point the electric field is almost independent of q, and therefore it mainly depends on $\bar{q}$. Figure 11 also represents the analytical fit (lines) obtained for the corresponding numerical values. For very small values of $\bar{q}$ we see that:

$$\eta_{ch}' \propto \bar{q}^s \tag{56}$$

with $0 < s < 1$, and therefore, in the limit $\bar{q} \to 0$ the electric field at ζ_{ch} becomes zero in the plasma-representation—i.e. $\eta_{ch}' \to 0$—but is singular in the Chodura-representation, i.e. $\partial_\zeta \tau|_{ch} = \bar{q}^{-1}\eta_{ch}' \propto \bar{q}^{s-1} \to \infty$. Both expressions (55) and (56) correspond to the boundary layer structure of the electric potential in the plasma-presheath and Chodura-layer regions on the one hand and the Chodura-layer and the sheath on the other.

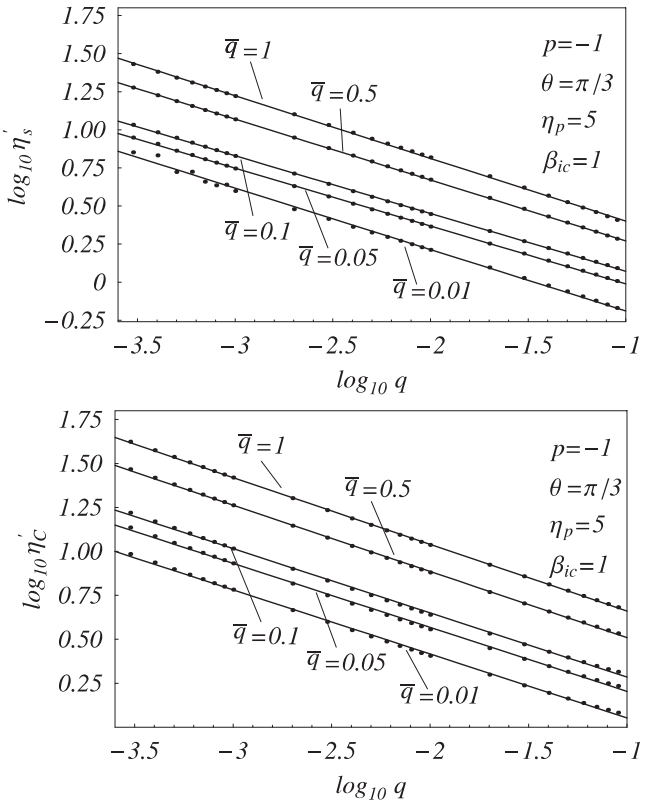

Figure 10. Electric field at the points ξ_s (where $\eta_0' \to \infty$) and the point $C \equiv \xi_C$ (where $u = 1$) calculated from the complete solution.

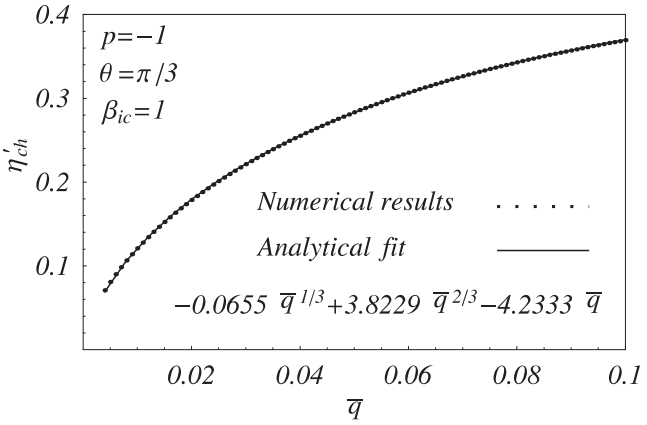

Figure 11. Electric field at the Chodura-edge ζ_{ch} and its analytical fit according to $\sum_{n\geqslant 1} a_n \bar{q}^{n/3}$.

4.4. A modified Bohm criterion for plasmas in the collisional regime does not exist

As mentioned in the introduction section, several authors have reported the idea that a new formulation of the Bohm criterion

for collisional plasmas exists. According to this formulation (see [13]), for the case of constant collision frequency ($p=-1$), the ion velocity normal to the wall at the sheath-edge would be limited by the upper and lower limit given by:

$$\left[\left(\frac{q_c}{2\dot{y}_s}\right)^2+1+\frac{q_b}{\dot{y}_s}v_s b_y\right]^{1/2}-\frac{q_c}{2\dot{y}_s}\leqslant u_s\leqslant\frac{\dot{y}_s}{q_c}+\frac{q_b}{q_c\,\dot{y}_s}v_s b_y \tag{57}$$

where $\dot{y}_s=\partial_X y|_s$ is the electric field at the sheath-edge X_s, obtained from the complete solution (these authors use the sheath-representation), where v_s is the y-component of the ion velocity at X_s, and $b_y=\sin\theta$. It is easy to show that even expressions like (57) are in agreement with the classical formulation of the Bohm criterion. As has been shown in [21] these kinds of expression are deduced from the misleading assumption that Sagdeev's potential has a maximum value at the sheath edge when $\lambda_D/\lambda_b\neq 0$. To show that (57) is in agreement with the Bohm criterion, we only have to consider the dependence of the electric field at the sheath-edge according to (55), that is $\dot{y}_s=q\eta'_s\propto q_b^r$, and therefore:

$$\begin{aligned}\frac{q_c}{\dot{y}_s}&\propto q_c q_b^{-r}=\beta_c q_b^{1-r}=\bar{f}_c\bar{q}q_b^{1-r}\\ \frac{q_b}{\dot{y}_s}&\propto q_b^{1-r}\\ \frac{q_b}{\dot{y}_s q_c}&\propto q_b^{1-r}q_c^{-1}=\frac{q_b^{-r}}{\beta_c}=\frac{q_b^{-r}}{\bar{f}_c\bar{q}}\end{aligned} \tag{58}$$

now, if we consider $\bar{q}$ and β_{ic} constant, when the non-neutrality parameter approaches zero $q_b\to 0$, (57) can be written as:

$$1+\ q_b^{1-r}\lesssim u_s\lesssim q_b^{1-r}+q_b^{-r} \tag{59}$$

and finally, in the marginal limit $q_b=0$ it yields:

$$1\leqslant u_s\leqslant\infty \tag{60}$$

which coincides with the original Bohm criterion.

4.5. *Drift term* $\mathbf{E}\times\mathbf{B}$

The action of a magnetic field in the plasma-sheath transition introduces a new presheath mechanism which is different from collisions and ionization. In this case, the physics behind the dynamics of the positive ions in addition to ionization and collisions corresponds to the drift velocity given by $\mathbf{v}_d=\mathbf{E}\times\mathbf{B}/B^2$. For a constant magnetic field strength, the drift term depends on the intensity of the electric field. Unlike collision or ionization, which act along the entire presheath region (plasma-presheath and Chodura-layer), the magnetic-presheath mechanism is only limited to the space region where the electric field (or E/B) becomes significant. This causes new boundary layer behaviour in the plasma-sheath transition associated with the breakdown of the collinearity of the ion velocity along the magnetic field lines, in the same way as the breakdown of quasineutrality—in the first case in a region which is very small compared with the plasma-presheath, and in the second case in a region (sheath) which is very small compared with the Chodura-layer.

In the case considered in this paper, magnetization is the dominant presheath mechanism, but not in the whole region from the plasma to the sheath. This is because in the plasma-presheath, the electric field is too weak, the drift term is negligible and the ion dynamics are dominated by collisions and/or ionization. In this region, where the electric field is too small, the ion fluid almost aligns with the magnetic field. In the Chodura-edge, the electric field increases and the drift term makes the ions deviate from the magnetic field to a direction perpendicular to the wall. The normalized drift velocity of the positive ions is given by:

$$\frac{v_d}{c_s}=\frac{|\mathbf{E}\times\mathbf{B}|}{c_s B^2}=\frac{\mathrm{d}\eta}{\mathrm{d}\xi}b_y \tag{61}$$

from (52) and (56), in the limit $\bar{q}\to 0$ the drift term in both the plasma-presheath region and at the Chodura-edge is zero,

$$\left.\frac{v_d}{c_s}\right|_{ch}\propto b_y\bar{q}^s\to 0 \tag{62}$$

and therefore, ions align with the magnetic field lines, even if $\lambda_b\gg\lambda_D$—i.e. the sheath is not magnetized.

5. Conclusions

This paper introduces a formalism based on what has been called the Chodura length scale for the case of a conducting wall immersed in a plasma under the action of a constant magnetic field, which helps us to introduce in a natural way the concepts of Chodura-representation, the Chodura-layer, the Chodura-edge and the Chodura-solution in a mathematical framework of boundary layer structure, when ionization and/or collisions are present. It is shown that the region from the plasma bulk to the wall can be divided into three: (i) the plasma-presheath, (ii) the Chodura-layer, and (iii) the sheath-region. At the Chodura-edge, which separates two quasineutral regions (the plasma-presheath and the Chodura-layer), the electric field has a singularity in the Chodura-representation as a consequence of the location of the magnetic presheath mechanism when the ion gyroradius is smaller than the mean free path for ionization and collisions. The thickness of the plasma-presheath, Chodura-layer, and the sheath has also been estimated. Finally we analyze the behaviour of the electric field at the Chodura-edge and the sheath-edge. This analysis allows us to show that (i) there is no modified Bohm criterion when collisions are introduced in the model, (ii) how the ion drift velocity corresponding to the magnetic presheath is only important in the Chodura-layer, and (iii) the ion velocity parallel to the magnetic field lines at the Chodura-edge can reach the sound speed, even for a weak magnetic field.

References

[1] Langmuir I 1923 The effect of space charge and initial velocities on the potential distribution and thermionic current between parallel plane electrodes *Phys. Rev.* **21** 419–35

[2] Allen J E 2009 The plasma-sheath boundary: its history and Langmuir's definition of the sheath edge *Plasma Sources Sci. Technol.* **18** 014004
[3] Chodura R 1982 Plasma-wall transition in an oblique magnetic-field *Phys. Fluids* **25** 1628–33
[4] Riemann K U 1994 Theory of the collisional presheath in an oblique magnetic-field *Phys. Plasmas* **1** 552–8
[5] Ahedo E 1997 Structure of the plasma-wall interaction in an oblique magnetic field *Phys. Plasmas* **4** 4419–30
[6] Stangeby P C 1995 The Bohm–Chodura plasma sheath criterion *Phys. Plasmas* **2** 702–6
[7] Sternberg N and Poggie J 2004 Plasma-sheath transition in the magnetized plasma-wall problem for collisionless ions *IEEE Trans. Plasma Sci.* **32** 2217–26
[8] Hutchinson I H 1996 The magnetic presheath boundary condition with exb drifts *Phys. Plasmas* **3** 6–7
[9] Kaouini M E, Chatei H, Driouch I and Hammouti M E 2011 Ion temperature effect on Bohm criterion for magnetized plasma sheath *J. Fusion Energy* **30** 199–204
[10] Kaouini M E and Chatei H 2012 Combined effect of ion temperature and magnetic field on collisionless sheath structure *J. Fusion Energy* **31** 317–24
[11] Hatami M M and Shokri B 2012 Bohm's criterion in a collisional magnetized plasma with thermal ions *Phys. Plasmas* **19** 083510
[12] Masoudi S F and Ebrahiminejad Z 2010 The sheath criterion for a collisional plasma sheath at the presence of external magnetic field *Eur. Phys. J.* D **59** 421–5
[13] Hatami M M and Shokri B 2013 Sheath formation criterion in magnetized electronegative plasmas with thermal ions *Phys. Plasmas* **20** 033506
[14] Ghomi H, Khoramabadi M, Shukla P K and Ghorannevis M 2010 Plasma sheath criterion in thermal electronegative plasmas *J. Appl. Phys.* **108** 063302
[15] Li J-J, Ma J X and Wei Z-A 2013 Sheath and boundary conditions in a collisional magnetized warm electronegative plasma *Phys. Plasmas* **20** 063503
[16] Crespo R M and Franklin R N 2014 Effect of an oblique and constant magnetic field in the sheath thickness, the floating potential and the saturation current collected by a planar wall *Plasma Sources Sci. Technol.* **23** 035012
[17] Allen J E 2008 The plasma boundary in a magnetic field *Contrib. Plasma Phys.* **48** 400–5
[18] Zimmermann T M G, Coppins M and Allen J E 2010 Coaxial discharge with axial magnetic field: demonstration that the Boltzmann relation for electrons generally does not hold in magnetized plasmas *Phys. Plasmas* **17** 022301
[19] Crespo R M, Ballesteros J, Fernandez J I, Hernandez M A, Diaz-Cabrera J M, Lucena-Polonio M V and Tejero-del A 2012 Boundary layer structure of the sheath surrounding a cylindrical or spherical probe in electronegative plasmas *Plasma Sources Sci. Technol.* **21** 055026
[20] Crespo R M, Ballesteros J, Palop J I F, Hernandez M A, Lucena-Polonio M V and Diaz-Cabrera J M 2011 Study of the electropositive to electronegative sheath transition in weakly ionized plasmas *Plasma Sources Sci. Technol.* **20** 7
[21] Crespo R M and Franklin R N 2014 Examining the range of validity of the Bohm criterion *J. Plasma Phys.* **80** 495–511